Time-lapse FWI prediction of CO_2 saturation and pore pressure

Qi Hu and Kristopher Innanen
Dept. of Geoscience, CREWES project, University of Calgary

SUMMARY

The estimation of CO_2 saturation and pore pressure from time-lapse seismic data requires a physical model relating the variations in reservoir properties to the changes in seismic attributes. We propose a complete rock physics workflow combing the modified Macbeth's relation and Gassmann's equation to predict elastic properties as a function of porosity, mineralogy, saturation, and pressure. We validate this workflow using a published dataset. In particular, we demonstrate the advantages of Macbeth's model in predicting the effect of pressure changes. Furthermore, we propose a full waveform inversion (FWI) algorithm incorporating the proposed model for predicting the time-evolution of CO_2 saturation and pore pressure. This approach allows for direct updating of reservoir properties from seismic data. We derive static rock properties, such as porosity and clay content, from baseline data and use them as input to predict dynamic reservoir properties (saturation and pressure) from monitor data. We illustrate the potential of the approach using a synthetic time-lapse dataset.

INTRODUCTION

An important technology supporting reduction of greenhouse gas emissions is the geological storage of carbon dioxide (Davis et al., 2019; Ringrose, 2020); Time-lapse seismic surveys provide a monitoring mode in which migration and distribution of the injected CO_2 can be tracked. Ideally, for reliable conformance verification, quantitative estimates/maps of CO_2 saturation and pore pressure would be produced by such technology, to be compared against reservoir modeling predictions (Dupuy et al., 2021).

In a previous study (Hu et al., 2023), we proposed a full waveform inversion (FWI) algorithm for predicting the spatial distribution of CO_2 saturation from time-lapse seismic data. The method is based on the application of a rock-physics parameterized FWI scheme that allows for direct updating of reservoir properties (Hu et al., 2021). In this simulation, the difference in pressure between the baseline and monitor stages is relatively small, so we assumed that the effect of pressure on seismic changes is negligible. For some fields or segments within a field, fluid and pressure changes affect the seismic data to about the same extent (Landrø et al., 2003). To cope with this situation, our proposed rock physics model and time-lapse FWI strategy must be adjusted to account for the pressure effect. With the fluid effect at seismic frequency being well described by Gassmann's equation (Mavko et al., 2020), the main challenge is the description of pressure within the rock physics model.

We first clarify the different types of geopressure. Pore pressure (P_p) is the pressure of fluids in the pore space of the rock.

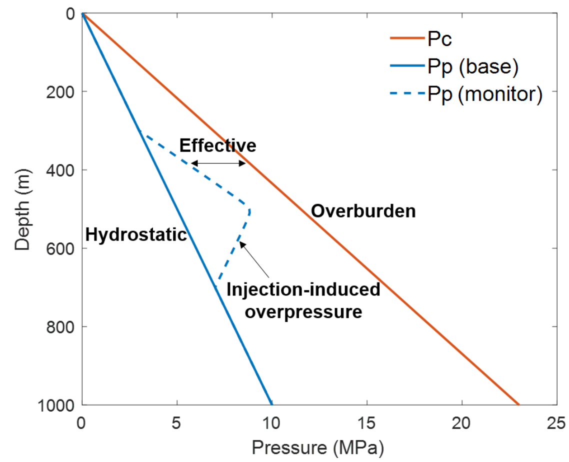

Figure 1: Example of different pressures with depth.

When pore pressure is hydrostatic, we have

$$P_p = \rho_w g z, \tag{1}$$

where z is the depth, g is the acceleration of gravity, and ρ_w is the density of water. When pore pressure exceeds the hydrostatic pressure, overpressure situation occurs. The confining or overburden pressure P_c results from the weight of overlying sediments and is generally obtained by integrating the density log:

$$P_c = g \int_0^z \rho(z')dz', \tag{2}$$

where ρ is the bulk density of the rock. Based on Terazaghi's (1965) principle, the effective pressure P_e is defined as the difference between overburden pressure and pore pressure:

$$P_e = P_c - P_p. \tag{3}$$

In Figure 1, we demonstrate the typical trends of these three pressures with depth, as well as possible overpressure anomalies due to CO_2 injection. Pore pressure and its development over time is a critical parameter for storage safety and it is also the main limiting factor for large-scale storage of CO_2 (Ringrose, 2020). However, since the effective pressure is more relevant to affecting the elastic properties of the rock, seismic pore pressure prediction is generally achieved by an accurate characterization of effective pressure on the assumption that overburden pressure is known. Similarly, although our inversion target is pore pressure, the key to this research is the modeling of effective pressure.

ROCK PHYSICS MODEL

An important criterion for us to choose a pressure model is whether it can be integrated into the entire modeling process based on the Gassmann's equation, because only in this way can the influence of other important parameters (such as porosity, lithology and fluid) on rock elastic properties be considered at the same time. Therefore, while there are many empirical formulas describing the relationship between velocity and effective pressure in the literature (Han, 1987; Eberhart-Phillips et al., 1989; Landrø, 2001; Jones, 1995; Sayers, 2006), these are outside the scope of our study.

In equations 4, the Gassmann's equation and density equation are given with underlined dependencies to the pressures and CO_2 saturation:

$$\begin{aligned} K_{\text{sat}} &= K_{\text{dry}}(P_e) + \frac{[1-K_{\text{dry}}(P_e)/K_m]^2}{\phi/K_f(S_{\text{co}_2},P_p)+(1-\phi)/K_m - K_{\text{dry}}(P_e)/K_m^2}, \\ \mu_{\text{sat}}(P_e) &= \mu_{\text{dry}}(P_e), \\ \rho_{\text{sat}}(S_{\text{co}_2},P_p) &= (1-\phi)\rho_m + \phi\rho_f(S_{\text{co}_2},P_p), \end{aligned} \tag{4}$$

where the subscripts $m, f, \text{dry}, \text{sat}$ indicate solid matrix, fluid phase, dry rock, and saturated rock, respectively. Based on the principle that effective pressure and pore pressure are interchangeable at a given overburden pressure, the effect of pressure on the elastic properties of saturated rock is due to its influence on the bulk modulus and density of fluid (K_f and ρ_f) and the elastic moduli of dry rock (K_{dry} and μ_{dry}). The former can be well described by the empirical formula proposed by Batzle and Wang (1992), while the latter requires more thought. An intuitive choice is a dry-rock theoretical model that includes a pressure term, such as the granular media models based on the Hertz-Mindlin contact theory. However, in a Hertz-Mindlin model, the dry-rock elastic modulus is proportional to the cube root of effective pressure, $K_{\text{dry}} \propto \sqrt[3]{P_e}$, which may be inconsistent with the exponential relationship revealed by various laboratory measurement data. After careful analysis, we focus on the modified MacBeth's equation proposed by Grana (2016).

MacBeth (2004) proposed an analogous equation to link dry-rock bulk modulus to effective pressure using an exponential relation:

$$K_{\text{dry}}(P_e) = \frac{K^{\infty}}{1 + A_K e^{-\frac{P_e}{P_K}}}, \tag{5}$$

where K^{∞}, A_K, and P_K are empirical parameters: K^{∞} represents the asymptotic value as effective pressure increases, whereas A_K and P_K are related to the curvature. Grana (2016) illustrated that K^{∞} and A_K are not independent if the dry-rock modulus K_0 at a given effective pressure P_0 is known, and modified Equation 5 to include dependence on porosity ϕ and clay content V_{clay}:

$$K_{\text{dry}}(P_e) = \frac{K^{\infty}}{1 + \frac{K^{\infty}-K_0}{K_0} e^{-\frac{P_{\text{eff}}-P_0}{P_K}}}; \tag{6}$$

$$K^{\infty} = \lambda_1(\phi + aV_{\text{clay}}) + \lambda_2, \tag{7}$$

where a, λ_1, and λ_2 are empirical parameters that must be fitted using lab measurements. Alternatively, datasets from literature or from nearby fields can be used to integrate the available core samples, as long as the observed pressure effect on elastic properties has the same behavior. Similar results have been obtained for the shear modulus:

$$\mu_{\text{dry}}(P_e) = \frac{\mu^{\infty}}{1 + \frac{\mu^{\infty}-\mu_0}{\mu_0} e^{-\frac{P_e-P_0}{P_\mu}}}; \tag{8}$$

$$\mu^{\infty} = \lambda_3(\phi + aV_{\text{clay}}) + \lambda_4, \tag{9}$$

where μ_0 is the dry-rock shear modulus at effective pressure P_0; λ_3 and λ_4 are empirical parameters.

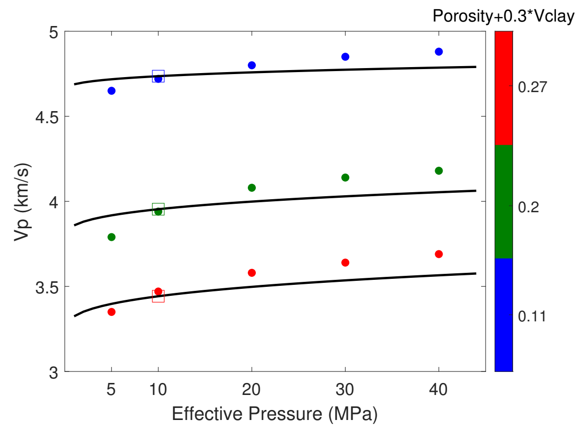

Figure 2: Calibration of rock physics model using Han's samples. The Hertz-Mindlin model is combined with Gassmann's equation to predict saturated-rock velocity as a function of effective pressure including porosity and mineralogy effects. The model is calibrated using baseline data with pressure 10 MPa, then automatically predicts the data at 5,20,30,40 MPa.

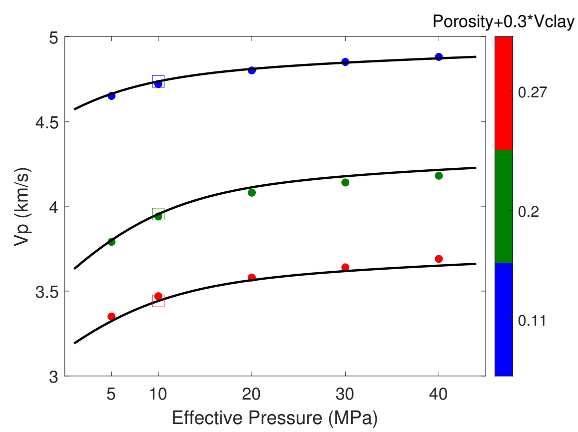

Figure 3: Modified Macbeth's relation combined with Gassmann's equation to predict saturated-rock velocity. The predicted data with Hertz-Mindlin equations at pressure 10 MPa are used as initial guess in Macbeth's model.

The modified MacBeth's equation focuses on the effect of pressure on elastic properties and are lack of mechanisms to account for the impact of rock properties, such as porosity and lithology. By contrast, the Hertz-Mindlin based models, although have a pressure term in their expressions, are classically used to predict static rock properties rather than pressure changes. To combine the advantages of both, we can use the modified MacBeth's equation as the dry-rock model for time-lapse study, but with the initial/baseline moduli, K_0 and μ_0, computed by the Hertz-Mindlin models.

Based on the above analysis, we propose a complete rock physics modeling process for CO_2 monitoring: 1) the mineral elastic moduli are computed using Voigt-Reuss-Hill average; 2) the fluid elastic moduli are computed using Brie's equation, assuming semi-patchy mixing of water and CO_2; 3) the dry-rock elastic moduli are calculated using the modified MacBeth's relation, in which the initial guess is provided by Hertz-Mindlin based models (e.g., soft-sand and stiff-sand models); 4) the fluid effect is included via Gassmann's equation to compute the elastic moduli of the saturated rock. 5) the density of the saturated rock is computed as a weighted average of the densities of mineral and fluid components. Consequently, we can express the velocity and density of the saturated rock as a function of porosity, mineral volumes, CO_2 saturation and pore pressure.

MODEL CALIBRATION

Here we take three samples from a published dataset of Han (1987) to illustrate how to calibrate the rock physics model in practical applications. Our goal is to calibrate the model so that it can accurately predict velocity as a function of porosity, clay content, and effective pressure. We assume that the initial pressure is 10 MPa, and that the data at other pressures correspond to the monitor survey. We first examine the model which uses Hertz-Mindlin model only. This means that once we calibrate the model at the initial pressure, the model automatically predicts the value at future pressures. Figure 2 shows that the Hertz-Mindlin model does not correctly approximate the nonlinear behavior of velocity due to pressure changes. On the other hand, the modified Macbeth's equation predicts the data accurately (Figure 3). In fact, the main advantages of this model are the exponential trend and the inclusion of empirical parameters that we can calibrate to match the observations.

TIME-LAPSE FWI STRATEGY

We modify the previous time-lapse FWI framework (Hu et al., 2023) to include one degree of freedom for the pore pressure. We first estimate the static rock properties, such as porosity (ϕ) and clay content (C) from baseline data ($\mathbf{d}_{\text{obs\_b}}$); we then use these baseline models as prior knowledge (fixed values) to estimate the dynamic properties, including CO_2 saturation (Sc) and pore pressure (P_p), from monitor data ($\mathbf{d}_{\text{obs\_m}}$). The objective functions for this problem are expressed as

$$E_b = \left\| \mathbf{d}_{\text{obs\_b}}(\phi^t, C^t) - \mathbf{d}_{\text{syn\_b}}(\phi, C) \right\|^2, \tag{10}$$

and

$$E_m = \left\| \mathbf{d}_{\text{obs\_m}}(\phi^t, C^t, Sc^t, {P_p}^t) - \mathbf{d}_{\text{syn\_m}}(\phi^b, C^b, Sc, P_p) \right\|^2. \tag{11}$$

NUMERICAL EXAMPLE

We apply the proposed approach to a synthetic model as shown in Figure 4. The initial CO_2 saturation is 0 everywhere and the initial pore pressure is hydrostatic. The two models then change locally due to the injection of CO_2 at 500 m depth and 500 m position. In this simulation, we neglect the uncertainty associated with the baseline model reconstruction. The details of the pressure model are illustrated in Figure 1, where we consider a clear pressure build-up due to the injection.

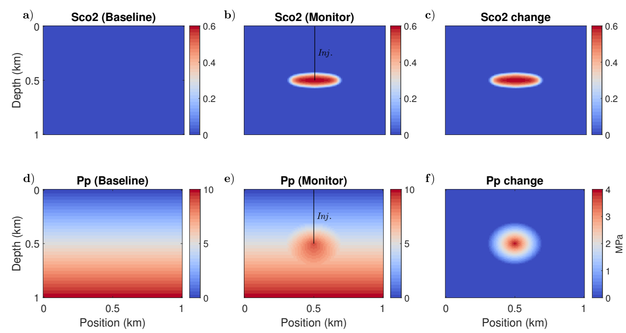

Figure 4: True baseline, monitor, and time-lapse models of CO_2 saturation and pore pressure. The black line indicates the location of the injection well.

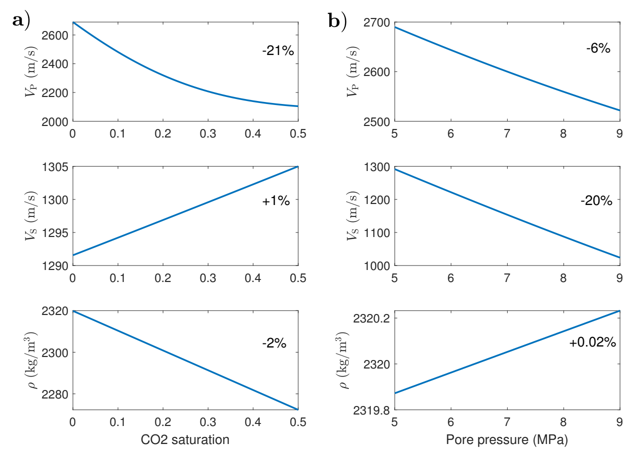

Figure 5: Theoretical curves of the proposed rock physics model: P-wave velocity, S-wave velocity, and density versus (a) CO_2 saturation and (b) pore pressure.

In Figure 5, we compute the theoretical curves of velocities and density as a function of CO_2 saturation and pore pressure based on the rock physics model. The results are consistent with existing studies: if CO_2 saturation increases, the P-wave velocity and density decrease, whereas the S-wave velocity slightly increases; both P- and S-wave velocities decrease as pore pressure increases, whereas the pressure effect on density is negligible.

In Figure 6, we plot the velocity and density models corresponding to the rock property model. The time-lapse elastic changes are consistent with the analysis in Figure 5. Consequently, we observe clear time-lapse events in the noise-free synthetic data (Figure 7). The recovered monitor model of CO_2 saturation and pore pressure are plotted in Figure 8, which shows a good agreement with the true models. The parameter crosstalk is weak. We attribute this to the fact that the two properties have very different sensitivities with respect to the P- and S-wave velocities (Figure 5). In Figure 9, the convergence properties of the inversion are summarized. We observe the convergence characteristics of a reliable inversion.

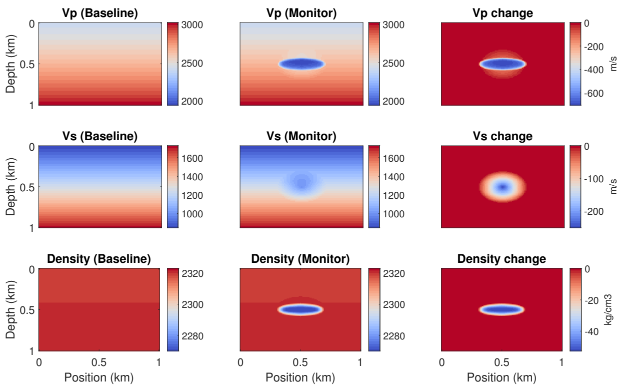

Figure 6: True baseline, monitor, and time-lapse models of P-wave velocity, S-wave velocity, and density.

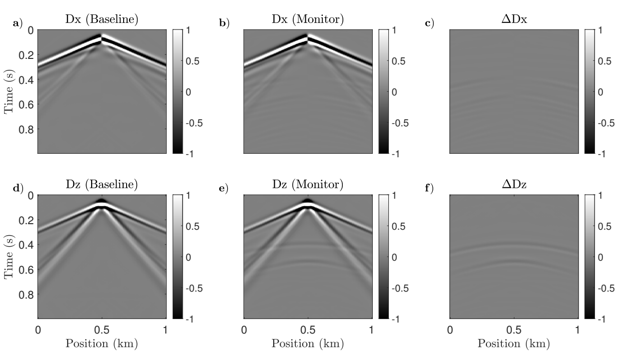

Figure 7: Baseline, monitor, and differential seismograms (horizontal and vertical displacements) computed for the true model. Ricker wavelet with central frequency 15 Hz is used.

Conclusions

We proposed a complete rock physics model for modeling saturation and pressure changes. A critical step in this model is the use of modified Macbeth's relation to account for the pressure effect on dry-rock elastic moduli. We then incorporate the rock physics model into an FWI algorithm for the quantitative prediction of CO_2 saturation and pore pressure from time-lapse seismic data. We demonstrate the effectiveness of this approach using a synthetic dataset. Examination of complex geological models and uncertainties associated with the rock physics model, the observed data, and the baseline inversion result are important steps in moving this research forward.

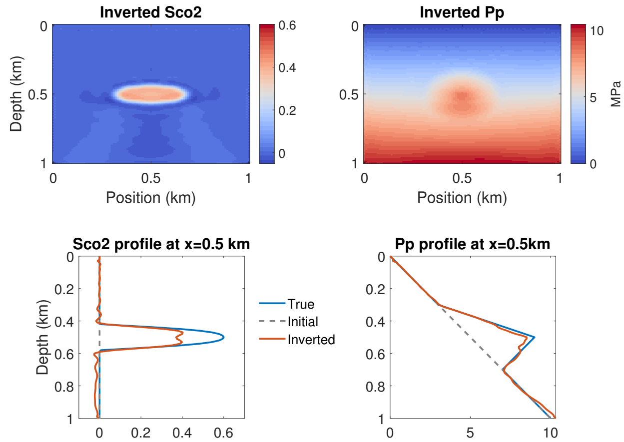

Figure 8: Recovered monitor model of CO_2 saturation and pore pressure.

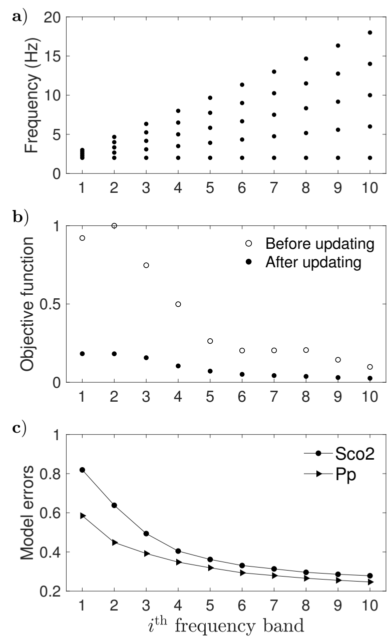

Figure 9: Convergence properties. (a-c) Frequencies, objective functions, and model errors (after updating) within a frequency band, respectively.

ACKNOWLEDGMENTS

This work was funded by CREWES industrial sponsors and NSERC (Natural Science and Engineering Research Council of Canada) through the grant CRDPJ 543578-19. The authors would like to thank Dario Grana (University of Wyoming) for insightful discussions.

REFERENCES

Batzle, M., and Z. Wang, 1992, Seismic properties of pore fluids: Geophysics, **57**, 1396–1408.

Davis, T. L., M. Landrø, and M. Wilson, 2019, Geophysics and geosequestration: Cambridge University Press.

Dupuy, B., A. Romdhane, P. Eliasson, and H. Yan, 2021, Combined geophysical and rock physics workflow for quantitative CO_2 monitoring: International Journal of Greenhouse Gas Control, **106**, 103217.

Eberhart-Phillips, D., D.-H. Han, and M. Zoback, 1989, Empirical relationships among seismic velocity, effective pressure, porosity, and clay content in sandstone: Geophysics, **54**, 82–89.

Grana, D., 2016, Pressure–velocity relations in reservoir rocks: Modified MacBeth's equation: Journal of Applied Geophysics, **132**, 234–241.

Han, D.-h., 1987, Effects of porosity and clay content on acoustic properties of sandstones and unconsolidated sediments: Stanford University.

Hu, Q., D. Grana, and K. A. Innanen, 2023, Feasibility of seismic time-lapse monitoring of co2 with rock physics parametrized full waveform inversion: Geophysical Journal International, **233**, 402–419.

Hu, Q., S. Keating, K. A. Innanen, and H. Chen, 2021, Direct updating of rock-physics properties using elastic full-waveform inversion: Geophysics, **86**, MR117–MR132.

Jones, S. M., 1995, Velocities and quality factors of sedimentary rocks at low and high effective pressures: Geophysical Journal International, **123**, 774–780.

Landrø, M., 2001, Discrimination between pressure and fluid saturation changes from time-lapse seismic data: Geophysics, **66**, 836–844.

Landrø, M., H. H. Veire, K. Duffaut, and N. Najjar, 2003, Discrimination between pressure and fluid saturation changes from marine multicomponent time-lapse seismic data: Geophysics, **68**, 1592–1599.

MacBeth, C., 2004, A classification for the pressure-sensitivity properties of a sandstone rock frame: Geophysics, **69**, 497–510.

Mavko, G., T. Mukerji, and J. Dvorkin, 2020, The rock physics handbook: Cambridge university press.

Ringrose, P., 2020, How to store CO_2 underground: insights from early-mover ccs projects: Springer.

Sayers, C. M., 2006, Sensitivity of time-lapse seismic to reservoir stress path: Geophysical prospecting, **54**, 369–380.

Terazaghi's, K., 1965, Theoretical soil mechanics: John Wiley and Sons.